VOL. 11, NO. 22, NOVEMBER 2016 ISSN 1819-6608
ARPN Journal of Engineering and Applied Sciences

www.arpnjournals.com

THE INFLUENCE OF ULTRASONIC TECHNIQUE ON THE GRADATION AND DEGRADATION MASS OF THE $Fe_{80}Cr_{20}$ ALLOY POWDER

A. M. Leman, Dafit Feriyanto, Winardi San, I. Baba and B. A Bakar
Faculty of Engineering Technology, Universiti Tun Hussein Onn Malaysia, Parit Raja, Batu Pahat, Johor, Malaysia
E-Mail: dafitferiyanto@yahoo.co.id

ABSTRACT

The main problem is the inevitable grain growth when metallic material operated in high temperature. Therefore, the main objective is to improve the thermal stability of $Fe_{80}Cr_{20}$ alloy for interconnect. The most promising technology to improve the properties by ultrasonic technique (UT). The materials was treated using ultrasonic with frequency of 35 kHz at various holding time of 3.5 h, 4.5 h and 5 h. Characterization and analysis were carried out by using Scanning Electron Microscope (SEM), Energy Dispersive X-Ray Spectroscopy (EDS) and Thermo Gravimetric Analysis (TGA). Ultrasonic technique can reduce the crystallite size from 138.656 nm to 37.477 nm, improve the finer surface morphology and more homogenous powder size as compared to untreated sample (raw material). Thermal stability was improved appropriate 9% when treated using ultrasonic technique at 4.5 h as compared to raw material. Therefore, that technique is required for improving the fine and homogenous powder size as well as thermal stability of $Fe_{80}Cr_{20}$ alloy as metallic material.

Keywords: homogenous, thermal stability, FeCr, ultrasonic technique.

INTRODUCTION

The $Fe_{80}Cr_{20}$ as metallic interconnect have several advantages such as easier machining, cheaper to fabricate, less brittle, easy to joined by simple technique (welding and brazing technique), high thermal conductivity and high thermal stability (Quadakkers *et al*., 2003). Interconnect should be fulfill a number of specific requirements under SOFC operating conditions such as high creep, oxidation resistance, reducing atmosphere, high thermal conductivity, high thermal stability and coefficient of thermal expansion (CTE) similar with the electrolyte and the electrodes (Quadakkers *et al.,* 2003), (Singhal and Kendall, 2003), (Stanislowski *et al*., 2007), (Palcut *et al.,* 2010). The interconnector must be stable in temperature more than 1000 ^{0}C because it is relatively operates at high temperature (Zhong and Mi, 2004). An interconnect is needed to connect the different thermal cells and also to provide physical barriers in order to keep the oxidant and fuel separated (Yaodong and Wei, 2007). Therefore, the metallic alloy which coupled by physical and mechanical properties is high recommended as SOFC interconnect based material. In addition, the metallic interconnect need to modify in order to improve in long term cell performance (Sebayang *et al*., 2011). The main problem in this study is how to minimize the grain growth in high temperature SOFC in order to reduce the negative impact in the system such as spalling which is caused by the metallic material forming the oxide scale during heat treatment (Sebayang *et al.*, 2011), (Montealegre *et al.,* 2005), (Young, 2008). One of the approached techniques is ultrasonic technique which not fully explored by previous researchers (Feriyanto *et al.,* 2014), (Juan and Juarez, 2010), (Krisztian and Daniel, 2010), (Puga *et al*., 2011). The ultrasonic technique is focused to increase the fine surface structure and homogenous of powder size which is factors that influence thermal stability enhancement of the metallic material in high temperature (Collins *et al*., 2006). It possess a great advantage because much wider range of specimen and geometries which could be evaluated. However, the material after consolidation process not completely control over the grain growth (Jerro *et al*., 1998), (Khalifaa *et al*., 2010). Therefore, it becomes the high challenge to modify the parameter of the ultrasonic technique such as the holding times of treatment which is promoted to reduce the crystallite size, improve the fine and homogeneous of the grain powders as well as improve the thermal stability.

METHODOLOGY

The $Fe_{80}Cr_{20}$ alloy powder as raw material means that the composition is 80 wt% Fe (320 mesh) and 20 wt% Cr (320 mesh). It selected because most corrosion resistance was observed at 20 wt% Cr in the FeCr alloys powder (Feriyanto *et al*., 2014). The several designation of the alloy material is listed in the Table-1.

Table-1. Designation of alloy materials.

Sample	Sample designation	Major features
$Fe_{80}Cr_{20}$	UT 0 h	Raw material/without ultrasonic technique
$Fe_{80}Cr_{20}$ 3.5 h	UT 3.5 h	Ultrasonic technique with holding time of 3.5 h
$Fe_{80}Cr_{20}$ 4.5 h	UT 4.5 h	Ultrasonic technique with holding time of 4.5 h
$Fe_{80}Cr_{20}$ 5 h	UT 5 h	Ultrasonic technique with holding time of 5 h

Ultrasonic technique

From the previous research (Feriyanto *et al*., 2014) ultrasonic was successfully conducted with holding time of 2.3 h and 3.5 h and frequency of 22 kHz and they successfully improve the homogeneity and fine surface structure in ultrasonic technique 3.5 h. Therefore, to improve the properties, this research is conducted using extended parameters by the frequency of 35 kHz and

various holding time of 3.5 h, 4.5 h, and 5 h in order to achieve more homogenous, finer surface and higher thermal stability properties. The specification (technical data) of the ultrasonic machine can be seen at the Table-2 and the ultrasonic machine is illustrated in Figure-1.

Table-2. Technical data of ultrasonic machine.

Description	Nominal
Bath dimension	Ø 24.5 cm and 13 cm deep
Effective capacity	5.6 liters
Insert tray	Ø 22.5, 11.5 cm deep with mesh 10 x 10 mm
Sound level	2 x 240 Watt/ period or 35 kHz
Power input	140 Watt
Weight	Net 5.5 kg, and gross 8 kg
Dimension w x d x h	27 x 27 x 27 cm

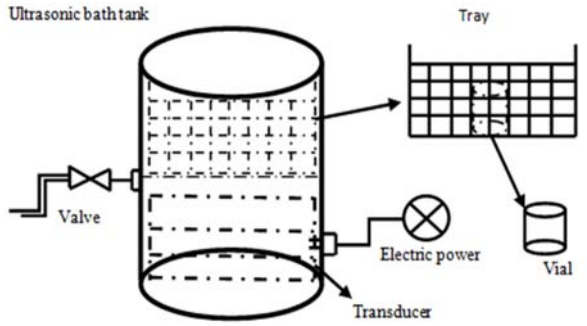

Figure-1. Ultrasonic machine (Feriyanto *et al*., 2014).

Microstructure and composition analysis

The microstructure and composition analysis were carried out by using Scanning Electron Microscopy (SEM) JEOL JSM-6380LA which equipped with Energy Dispersive x-ray Spectroscopy (EDS). SEM and EDS were carried out to obtain the surface structure, chemical composition and to identify the microstructure and phase constitution of scale or internal oxides (Deni, 2011). SEM have many advantages for examining surface material such as high resolutions 1-5 nm, large depth of focus, possibility to microanalysis, low and high magnification (about 15 to 100 000 times). The analysis was conducted with the magnification of 1000 times, voltage of 15 kV and WD of 7.5 mm.

Determination of crystallite size

Crystallite size of $Fe_{80}Cr_{20}$ alloy is calculated by using Williamson-Hall formula that assuming both size and strain broadened profile is similar nature (Choudhury and Sarma, 2011). Williamson-hall size-strain analysis was developed in 1953 as a method to separate size and strain effect by their angular dependence (Ungar *et al*., 2001), (Mittemeijer and Welzel, 2008). Williamson-Hall formula is shown in equation (1).

$$\partial(2\theta)Cos\theta = \frac{0.9\lambda}{D_{WH}} + 4\varepsilon Sin\theta \quad (1)$$

Where; D = The crystallite size

$\partial(2\theta)$ = FWHM (radians)

ε = Strain of material

θ = Diffraction angle (^{0})

λ = Wavelength

Thermal analysis

Thermal analysis was conducted using Thermo Gravimetric Analysis (TGA). TGA measure mass changes of the samples as a function of temperature or time in atmospheric environment. Mass change phenomena due to gas absorption, gas desorption, phase transition and for chemical such as decomposition, break down reaction, gas reaction, and chemisorptions (Linda, 2013). TGA was carried out in temperature of 900 ^{0}C which starting from 20 ^{0}C with heating rate of 10 ^{0}C and also cooling rate of 10 ^{0}C. TGA machine located at polymer and ceramic laboratory UTHM.

RESULTS AND DISCUSSIONS

Significant differences of the surface morphology, particle size and homogeneity of $Fe_{80}Cr_{20}$ alloys as shown in Figure-2. Finer surface structure and homogeneity of particle size is produced after ultrasonic technique. However, the agglomeration still observed due to the overlapping was occurred between particles during ultrasonic process (Deni, 2011).

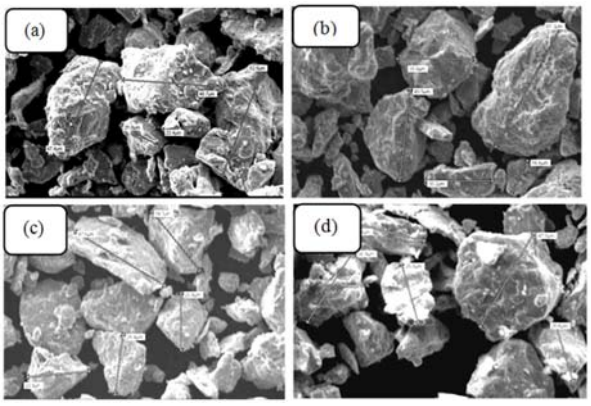

Figure-2. SEM analysis (a): UT 0 h, (b): UT 3.5 h, (c): UT 4.5 h, (d): UT 5 h.

Increasing holding time is led to finer surface as well. One of the techniques for measuring particle size by using SEM which counted particle sizes of each parameter are (a): 39.98 µm, (b): 37.48 µm, (c): 23.98, and (d): 35.22 µm. The higher reducing particle size after treatment is located at holding time of 4.5 h. Meanwhile, when measurement is carried out using Williamson-hall formula, the crystallite size of each parameter is (a): 138.656 nm, (b): 57.776 nm, (c): 37.477 nm and (d): 37.991 nm as listed in Table-3. Smaller crystallite size is produced because the

frequency as the shock wave throughout the liquid and hit the particle mass which led to high-speed collisions between particles.

Table-3. Crystallite size and strain of the sample with ultrasonic technique.

Sample designation	D (nm)
UT 0 h	138.656
UT 3.5 h	57.776
UT 4.5 h	37.477
UT 5 h	37.991

The EDS analysis was conducted on the sample designation for counting amount of impurities or contaminant of individual particle of iron and chromium powder. It known by EDS spectrum of the treated and untreated samples which is shown in Figure-3. The EDS indicated that iron and chromium with high concentration in the surface region of particle.

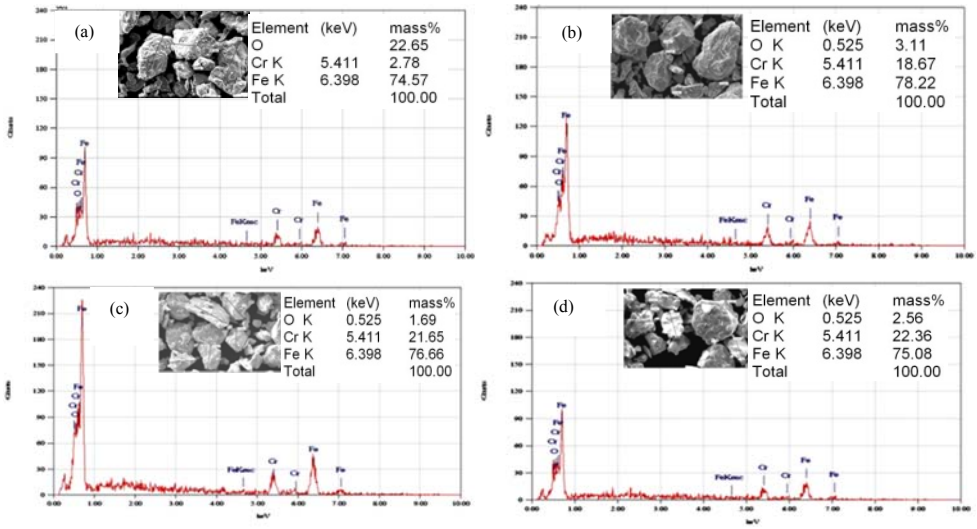

Figure-3. EDS result of (a) UT 0 h; (b) UT 3.5 h; (c) UT 4.5 h and (d) UT 5 h.

The concentration of the Fe and Cr after treatment process is quite closer to $Fe_{80}Cr_{20}$ than untreated sample which shown in Figure-3. It shows the oxygen was reduced by ultrasonic treatment. Meanwhile, in Figure-3(a) shows that the higher oxygen was observed due to the powder mixed manually at 1-2 minutes. Ultrasonic technique breaks the alloy powder using the shock out waves or high speed bubbles which can reduce the oxygen cavities. However, the oxygen still observed in EDS analysis because the analysis was conducted in atmospheric environment before the sample filled to the jar. In addition, the presence of the oxygen in the $Fe_{80}Cr_{20}$ alloy promote to easily form the Cr_2O_3 scale at temperature over of 500 ^{0}C. Therefore, it can be promoted to develop higher oxidation and corrosion resistance in high temperature. The point of reaction and weight change derivative of the treated and untreated samples as listed in Table-4 and Table-5, respectively.

Table-4. Point of reaction in TGA.

Sample designation	Point of reaction (mg/min)	Temperature (^{0}C)
UT 0 h	0.91	735.2
UT 3.5 h	0.87	752.15
UT 4.5 h	0.81	780.65
UT 5 h	0.87	753.05

Table-4 shows that the maximum mass changes as a function of time which called as point of reaction. Highest point of reaction shown by untreated (UT 0 h) sample at 0.91 mg/min at temperature of 735.2 ^{0}C. Higher point of reaction at the lower temperature means that the sample have lower thermal stability due to the material have the maximum oxidation at low temperature. Larger crystallite size and less homogenous powder size of UT 0 h than treated samples led to the samples generates higher point of reaction at lower temperature. Table-5 shows that there are

two various reaction which are oxidation and reduction phase. Oxidation was occurred when the $Fe_{80}Cr_{20}$ alloy formed with oxygen or the oxygen bonding was occurred (Suparni, 2009). Meanwhile, the reduction was occurred when the oxygen released by the $Fe_2O_{3(s)} + Cr_2O_{3(s)}$ element. Reduction may be due to the hydrogen gas reacts in the $Fe_{80}Cr_{20}$ alloy (Suparni, 2009).

Table-5. Mass changes derivative of the treated and untreated samples.

Temperature (^{0}C)	Sample designation	Mass change derivative (mg/^{0}C)
4.4-9.9	UT 0 h	-0.00135
	UT 3.5 h	-0.0068
	UT 4.5 h	-0.00425
	UT 5 h	-0.003
552-572	UT 0 h	0.07005
	UT 3.5 h	0.06505
	UT 4.5 h	0.06665
	UT 5 h	0.0662
738-805	UT 0 h	0.09115
	UT 3.5 h	0.08725
	UT 4.5 h	0.08175
	UT 5 h	0.0866
900	UT 0 h	0.0384
	UT 3.5 h	0.03305
	UT 4.5 h	0.04165
	UT 5 h	0.0328

Highest mass change derivative of 0.09115 mg/^{0}C is located at UT 0 h which occurred at a temperature of 735-805 ^{0}C as shown in Table-5. Higher reduction of the last steps (at 900 ^{0}C) means the material still has endurance to heat treated or higher thermal stability as shown in UT 4.5 h samples with the mass changes derivative of 0.04165 mg/^{0}C. Meanwhile, lower reduction at temperature of 900 ^{0}C means the samples start to leave the elastic phase towards plastic areas or failure condition. Mass gain of the treated and untreated samples is shown in Figure-4 where the lowest mass gain of 24 mg is located at UT 4.5 h. Mass change measurement with higher ultrasonic time could measured using the equation in Figure-4.

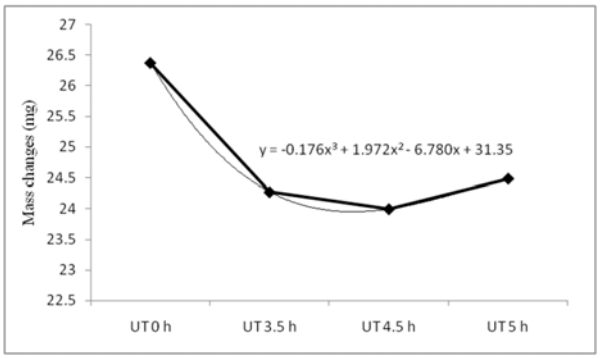

Figure-4. Mass changes of treated and untreated sample.

The mass change of the treated samples is smaller as compared to untreated samples. According to the results of crystallite size, SEM and EDS analysis, smaller crystallite size, finer surface morphology and more homogenous powder size effect to the higher thermal stability. Highest mass gain is shown by UT 0 h of 26.37 mg and the mass gain start to increase which is located at UT 5 h. It is due to during the shock out wave through the liquid, hit the powder caused temperature increased which led to the materials that receive plastic deformation increased. Mass change derivative curves are shown in Figure-5 which is showing 2 times experiment in order to validate the results. In the early stage the degradation was occurred due to buoyancy of the sample cup in the TGA machine and influenced by CO_2 which produced by atmospheric condition (Ranjani *et al.*, 1999) and then followed by normal curves.

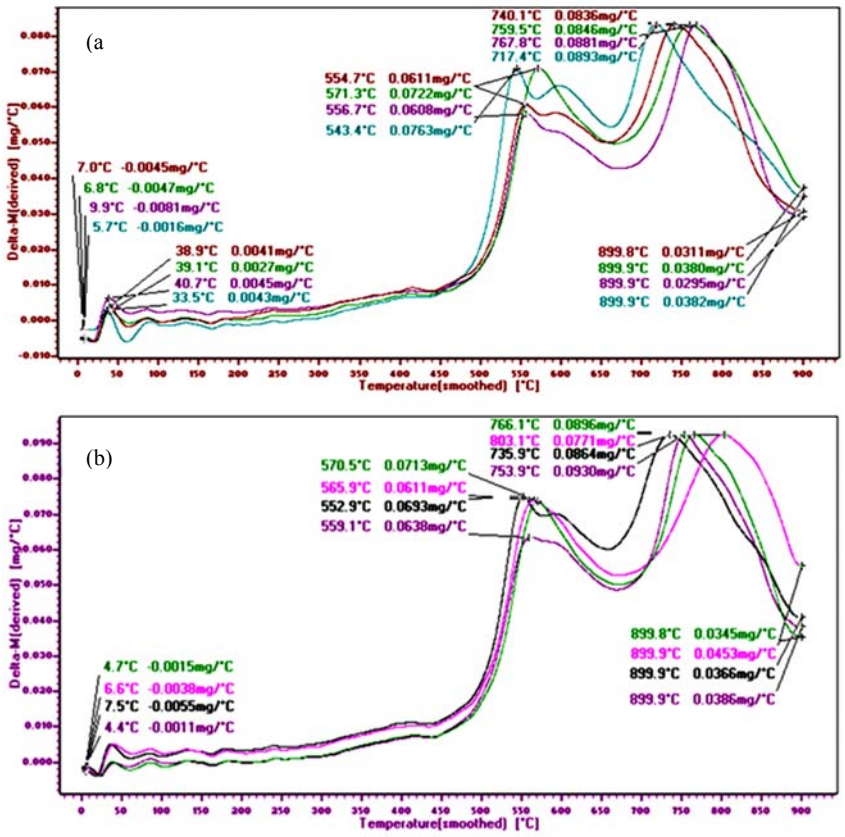

Figure-5. Comparison of mass change derivative (a) for first test and (b) for second test.

Figure-5 shows the fluctuate condition during TGA process which consist of gradation (oxidation) and degradation (reduction) phase. Gradation phase occurred when the mass change derivative is increased as shown in temperature of 300-571^{0}C and 670-803 ^{0}C. Meanwhile the reduction is occurred when the mass change derivative decreased as shown in temperature of 572-669 ^{0}C and 804-900 ^{0}C. The average data of two times experiments as listed in Table-5.

CONCLUSIONS

Producing high thermal stability, fine surface and homogenous powder could be conducted by several techniques. One of those techniques is using ultrasonic technique which successfully done to achieve that properties. Finer surface and closer composition to the compound of 21.65 wt% Cr and 76.65 wt% Fe obtained in ultrasonic treatment samples at 4.5 h. Higher thermal stability of 9% shown by treated samples when compared to untreated sample which shown that ultrasonic technique is recommended to improve the sample properties. However, need more exploration of the ultrasonic parameter to achieve the advance results.

ANKNOWLEDGEMENT

The authors would like to thank the Ministry of Higher Education Malaysia and Universiti Tun Hussein Onn Malaysia (UTHM) through the FRGS grant with Vot No. 1216 and CGS – UTHM.

REFERENCES

Quadakkers, W.J., Piron, A.J., Shemet, V. and Singheiser, L. 2003. Metallic interconnector for solid oxide fuel cells-a review. Forchungzentrum Julich, 2, pp. 115-127.

Singhal, S.C. and Kendall, K. 2003. High-Temperature Solid Oxide Fuel Cells: Fundamentals, Design and Applications; Oxford, UK: Elsevier.

Stanislowski, M., Froitzheim, J., Niewolak, L., Quadakkers, W.J., Hilpert, K., Markus, T. and Singheiser, L. 2007. Reduction of chromium vaporization from SOFC interconnectors by highly effective coatings. J. Power Sources, 164, p. 578.

Palcut, M., Mikkelsen, L., Neufeld, K., Chen, M., Knibbe, R. and Hendriksen, P.V. 2010. Corrosion stability of ferritic stainless steels for solid oxide electrolyser cell interconnects. Corros.Sci., 52, pp. 3309--3320.

Zhong, Z.W. and Mi, Y. 2004. Perspectives on the metallic interconnect for solid oxide fuel cells. Journal Of Zhejiang University-Science A., 5(12), pp. 1471-1503.

Yaodong, L. and Wei, L. 2007. Mechanical alloying and spark plasma sintering of the intermetallic compound $Ti_{50}Al_{50}$. Journal of Alloys and Compounds, 440, pp. 154-157.

Sebayang, D., Deni, S.K., Saryanto, H., Omar, B., Othman, M.A., Hamid, A., Sujitno, T. and Untoro, P. 2011. Oxidation resistance of unimplanted and implanted of nanocrystalline FeCr alloy and commercial alloy with lanthanum. Journal of Advanced Microscopy Research, 6, pp. 1-15.

Montealegre, M.A., Strehl, G., Gonzales-Carassco, J.L. and Borchardt, G. 2005. Oxidation behaviour of novel ODS FeCrAl intermetallic alloys. Intermetallics, 13, p. 896.

Young, D.J. 2008. High temperature oxidation and corrosion of metals. Elsevier Corrosion Series; Oxford, UK: Elsevier.

Feriyanto, D., Izwana, M.I., Sebayang, D., Ashraf, O. and Untoro, P. 2014. Microstructure study on Fe/Cr based alloys added with yttrium oxide (Y_2O_3) prepared via ultrasonic technique for Solid Oxide Fuel Cell (SOFC) application. Applied Mechanics and Materials, 493, pp. 651-655, ISSN: 1662-7482.

Juan, A. and Juarez, G. 2010. High-power ultrasonic processing: recent developments and prospective advances. Physics Procedia, 3, pp. 35-47.

Krisztian, N. and Daniel, E.M. 2010. Sonication-accelerated catalytic synthesis of oxide nanoparticles. Nano Today, 5, pp. 99-105.

Puga, H., Costa, S., Barbosa, J., Ribeiro, S. and Prokic, M. 2011. Influence of ultrasonic melt treatment on microstructure and mechanical properties of $AlSi_9Cu_3$ alloy. Journal of Materials Processing Technology, 211, pp. 1729--1735.

Collins, C., Lucas, J., Buchanan, T. L.. Kopczyk, M., Kayani, A., Gannon, P.E., Deibert, M.C., Smith, R.J., Choi, D.S. and Gorokhovsky, V.I. 2006. Surface Coating Technology, 201, p. 4467.

Jerro, W.L., Laurence, J.J. and abdulhamid, Z. 1998. Ultrasonic technique to characterize pultruded composite members. Journal of Composite for Construction.

Khalifaa, W., Tsunekawab, Y. and Okumiya, M. 2010. Effect of ultrasonic treatment on the Fe-intermetallic phases in ADC12 die cast alloy. Journal of Materials Processing Technology, 210, pp. 2178-2187.

Deni, S.K. 2011. Development of nanocrystalline iron-chromium alloy by means of sintering and ion implantation for interconnect application in high temperature solid oxide fuel cells. Master Thesis, Fac. Mechanical Engineering and Manufacturing Engineering. Universiti Tun Hussein Onn Malaysia, Malaysia.

Choudhury, N. and Sarma, B.K. 2011. Structural analysis of chemically deposited nanocrystalline PbS films. Journal of Thin Solid Films, 519, pp. 2132-2134.

Ungar, T., Gubicza, J., Ribaarik, G. and Borbealy, A. 2001. Aqueous chemical growth of alpha-Fe_2O_3 alpha- Cr_2O_3 Nanocomposite thin films. Journal of Nanoscience Nanotechnology, 1(4), pp. 385-388.

Mittemeijer, E.J. and Welzel, U. 2008. The state of the art of the diffraction analysis of crystallite size and lattice strain. J. Kristallogr, 233, pp. 552-560.

Linda, F. 2013. Thermal analysis TGA / DTA. Abo Academy University.

Suparni, S.R. 2009. Chemical process on high furnace. RSS Article.

Ranjani, Siriwardane, V., James Jr. A.P., Edward, P.F., Shen, M.S. and Angela, L.M. 1999. Decomposition of the sulfates of copper, iron (II), iron (III), nickel, and zinc: XPS, SEM, DRIFTS, XRD, and TGA study. Journal of Applied Surface Science, 152, pp. 219-236.